

# Some size-dependent electronic properties in charged MgO clusters

C. Coudray<sup>a</sup> and G. Blaise

Laboratoire de Physique des Solides, Université Paris-Sud, Bâtiment 510, 91405 Orsay, France

Received 9 September 2002 / Received in final form 17 March 2003

Published online 12 August 2003 – © EDP Sciences, Società Italiana di Fisica, Springer-Verlag 2003

**Abstract.** Starting from two cubic pieces of a MgO crystal ( $(3 \times 3 \times 3)$  and  $(5 \times 5 \times 5)$ ), both containing a central oxygen atom, two clusters are simulated with the help of a DFT-LDA method. These clusters are charged in order to be equivalent to pieces of a neutral crystal. In each cluster, a neutral vacancy analogous to a F center is created by removing the central oxygen atom. Then,  $F^+$  and  $F^{++}$  centers are simulated by removing one and two electrons. The main differences and similarities between the two sizes of clusters are studied: geometries, Mulliken charges, electronic distributions, gaps, ionisation potentials. An important result is that in any case, when a F center is simulated, the vacancy does not accept more than about one electron, the second one being spread in the rest of the cluster.

**PACS.** 31.15.Ar Ab initio calculations – 36.40.Wa Charged clusters – 61.72.Ji Point defects (vacancies, interstitials, color centers, etc.) and defect clusters

## 1 Introduction

The study of clusters is one of the most stimulating topics in to-day physics, not only for their intrinsic properties, but also because they pave the way between microscopic and macroscopic objects. Metallic clusters have been extensively studied and have shown size-dependent regularities which, in some respects, can be compared to those of nuclei [1]. The study of oxide clusters is more recent [2–27], and much work remains to do in order to have access to a thorough knowledge of their main properties. Amongst the unsolved questions, an important one is that of their electronic distribution, in particular when they are positively or negatively charged. In a previous study [27], we showed that the ionicity of small neutral oxide clusters is size-dependent. Is this property still true when the clusters are charged? And is it possible to deduce from the study of clusters a microscopic understanding of the charging process of an oxide crystal?

In this paper we give elements of answer to these questions by the simulation of charged MgO clusters. The chosen clusters are built from cubic pieces of MgO crystal with a central oxygen atom: either  $(3 \times 3 \times 3)$  cubes (small clusters), or  $(5 \times 5 \times 5)$  cubes (large clusters). In both cases, the central oxygen atom is suppressed, leading to vacancy clusters. According to the charge the removed oxygen atom carries away, one or two electrons are likely to remain in the vacancy cluster. For each cluster size, the

location of these electrons is looked for, and a comparison is done between the two sizes.

Apart from its intrinsic interest relative to clusters, this study has a natural extension in the charging of a vacancy in a MgO crystal. In fact, the methods of simulation usually chosen for crystals, methods which have recourse to periodic wave functions, are difficult to handle when the crystal presents a defect. A simulated crystal possessing vacancies in a periodic way has perhaps not the same properties than a crystal with a unique vacancy. Besides, if each vacancy could bear a charge, the total charge of such a crystal would be infinite, unless a subtraction method included in the computation [28–31].

On the other hand, the extrapolation to the crystal of results obtained from clusters is delicate due to the problem of the limiting surfaces. A better method would be perhaps to embed the cluster in a continuous medium reproducing the polarisability properties of the crystal, as proposed a long time ago by Lorentz (Lorentz sphere). However the frontier between the cluster and this medium is difficult to set up; an abrupt frontier would make the results subject to caution. Another method, frequently used, consists in embedding the cluster in an environment which simulates the rest of the crystal: most frequently an array of point charges [7, 19, 20] or of shell-model ions [6, 8] placed at the lattice positions, but sometimes more complicated arrangements [18, 21, 24]. This environment can be adjusted during the simulation [21]. It is not obvious that these structures give better results in the vicinity of the vacancy than that obtained from raw pieces of crystal, choice which is deliberately done in this paper. The results

---

<sup>a</sup> e-mail: coudray@lps.u-psud.fr

we obtain indicate that an extrapolation to the crystal can be done from only large enough clusters.

## 2 The numerical procedure

The computations have been made with the code DMol based on the theory of the functional density in the local density approximation (DFT-LDA theory) [32,33]. This code, introduced about ten years ago by Delley, was extensively described in his papers [34,35]. It works in two steps. A first step is devoted to the energy minimisation of a molecule of given geometry; this energy minimisation is obtained by a repartition of the electronic density. The second step consists of a slight modification of the geometry according to the forces the electronic density exerts on atoms. A new energy minimisation occurs, and the process begins again. It stops when both energy variations and either forces or displacements become less than  $10^{-5}$  a.u.

The basis chosen in this study is exactly the same as that described in reference [26]. Similarly, the exchange and correlation energy has been estimated in the approximation of Hedin and Lundqvist [36]. The Oh symmetry is chosen for all clusters. This choice, which excludes the possibility of Jahn-Teller effects, agrees with many experimental results [4,5,9–11] which seem to indicate that MgO clusters keep the crystal symmetries. Besides, starting from somewhat asymmetrical structures, we tried to minimise them without imposing any symmetry; in any case our simulations led to clusters possessing the Oh symmetry.

## 3 Charging the clusters

In a crystal, the electric neutrality requires an equal number of positive and negative charges, which is obtained in MgO by an equal number of anions and cations. The clusters obtained from either a  $(3 \times 3 \times 3)$ , or a  $(5 \times 5 \times 5)$  crystal cube involving an oxygen atom in its center are respectively  $[(\text{MgO})_{13}\text{Mg}]$  and  $[(\text{MgO})_{62}\text{O}]$ . In the first one, one magnesium atom is in excess and two electrons stand in the conduction band. In the second one, two empty states belonging to the excess oxygen atom appear in the valence band. In order to simulate clusters electronically equivalent to pieces of a neutral crystal, two electrons have to be removed in the first cluster, and added in the second one, giving rise to  $[(\text{MgO})_{13}\text{Mg}]^{2+}$  and  $[(\text{MgO})_{62}\text{O}]^{2-}$ . These clusters are shown in Figure 1.

When an oxygen atom is removed in a neutral state, two filled  $2p$  oxygen states disappear and are replaced by two filled states in the bandgap:  $[(\text{MgO})_{12}\text{Mg}_2\text{V}_0]^{2+}$  and  $[(\text{MgO})_{62}\text{V}_0]^{2-}$  are equivalent to a neutral crystal with a neutral vacancy (F center). Instead of a neutral oxygen atom, an oxygen ion can be removed. As previously, two filled  $2p$  states are suppressed and two states appear in the gap. If  $\text{O}^{2-}$  is removed, these states are both empty, one of them is filled if  $\text{O}^-$  is removed. One then obtains either  $[(\text{MgO})_{12}\text{Mg}_2\text{V}_0]^Q$  ( $Q = +3, +4$ ) or  $[(\text{MgO})_{62}\text{V}_0]^Q$

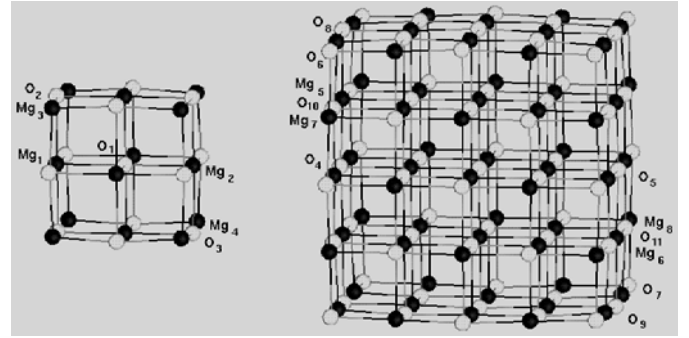


**Fig. 1.** The clusters  $[(\text{MgO})_{13}\text{Mg}]^{2+}$  (left-hand side) and  $[(\text{MgO})_{62}\text{O}]^{2-}$  (right-hand side). The white spheres are the oxygen atoms, the black spheres the magnesium atoms.

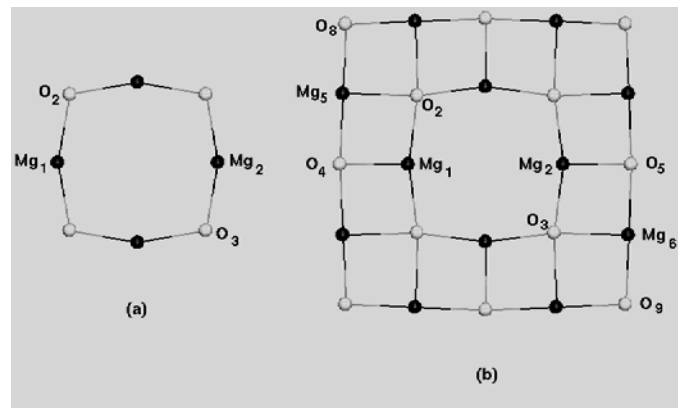


**Fig. 2.** Central (100) planes of (a)  $[(\text{MgO})_{12}\text{Mg}_2\text{V}_0]^{4+}$  and (b)  $[(\text{MgO})_{62}\text{V}_0]^0$ . In these clusters, the vacancies are equivalent to  $\text{F}^{++}$  centers. The white spheres are the oxygen atoms, the black spheres the magnesium atoms.

( $Q = -1, 0$ ), equivalent to  $\text{F}^+$  and  $\text{F}^{++}$  centers (positively charged vacancies in a crystal).

Similarly, adding electrons to a cluster equivalent to a neutral crystal provides a cluster equivalent to a negatively charged crystal. The equivalences between crystal and clusters are given in Table 1.

In this paper we concentrate on clusters equivalent to neutral and positively charged crystals.

## 4 Clusters geometries

Non-vacancy clusters possess a certain sphericity (*cf.* Fig. 1), increased by the removal of the central atom and by that of electrons. For instance, Figure 2 represents the central (100) planes of  $[(\text{MgO})_{12}\text{Mg}_2\text{V}_0]^{4+}$  and of  $[(\text{MgO})_{62}\text{V}_0]^0$ , obtained by creation of a vacancy equivalent to a  $\text{F}^{++}$  center in the clusters of Figure 1.

In order to compare the clusters geometries, one first defines the ratio  $\rho_{A_i A_j}$  as:

$$\rho_{A_i A_j} = \frac{(d_{A_i A_j})_{\text{cluster}}}{(d_{A_i A_j})_{\text{crystal}}}$$

**Table 1.** Charge equivalence between the two sizes of clusters, the crystal being taken as a reference.

neutral non-vacancy crystal	$[(\text{MgO})_{13}\text{Mg}]^{2+}$	$[(\text{MgO})_{62}\text{O}]^{2-}$
neutral vacancy crystal (F center)	$[(\text{MgO})_{12}\text{Mg}_2\text{V}_0]^{2+}$	$[(\text{MgO})_{62}\text{V}_0]^{2-}$
[vacancy crystal] <sup>1+</sup> (F <sup>+</sup> center)	$[(\text{MgO})_{12}\text{Mg}_2\text{V}_0]^{3+}$	$[(\text{MgO})_{62}\text{V}_0]^{1-}$
[vacancy crystal] <sup>2+</sup> (F <sup>++</sup> center)	$[(\text{MgO})_{12}\text{Mg}_2\text{V}_0]^{4+}$	$[(\text{MgO})_{62}\text{V}_0]^0$

**Table 2.** Values of the interatomic distances  $d_{A_1A_2}$  of the quantities  $\rho_{A_1A_2}$ , and of the sphericities  $s$  in the crystal and in the clusters. All distances are given in Å. See Figure 1 for the locations of the atoms. For the vacancy clusters, the equivalent defect in a crystal is indicated in the second column (see Tab. 1).

	$d_{\text{Mg}_1\text{Mg}_2}$	$\rho_{\text{Mg}_1\text{Mg}_2}$	$d_{\text{O}_2\text{O}_3}$	$\rho_{\text{O}_2\text{O}_3}$	$d_{\text{Mg}_3\text{Mg}_4}$	$\rho_{\text{Mg}_3\text{Mg}_4}$	$s$	$d_{\text{O}_4\text{O}_5}$	$\rho_{\text{O}_4\text{O}_5}$	$d_{\text{O}_6\text{O}_7}$	$\rho_{\text{O}_6\text{O}_7}$	$s$
Crystal	4.22		5.97		7.31		0	8.44		14.62		0
$[(\text{MgO})_{13}\text{Mg}]^{2+}$	4.07	0.965	5.76	0.965	6.63	0.907	0.06					
$[(\text{MgO})_{12}\text{Mg}_2\text{V}_0]^{2+}$ F	4.44	1.05	5.64	0.945	6.66	0.911	0.13					
$[(\text{MgO})_{12}\text{Mg}_2\text{V}_0]^{3+}$ F <sup>+</sup>	4.52	1.07	5.60	0.938	6.68	0.914	0.15					
$[(\text{MgO})_{12}\text{Mg}_2\text{V}_0]^{4+}$ F <sup>++</sup>	4.62	1.095	5.55	0.93	6.70	0.917	0.163					
$[(\text{MgO})_{62}\text{O}]^{2-}$	4.08	0.967	5.72	0.96	6.96	0.95	0.02	8.28	0.98	13.68	0.936	0.045
$[(\text{MgO})_{62}\text{V}_0]^{2-}$ F	4.14	0.98	5.72	0.96	6.97	0.95	0.03	8.28	0.98	13.68	0.936	0.045
$[(\text{MgO})_{62}\text{V}_0]^{1-}$ F <sup>+</sup>	4.29	1.017	5.66	0.948	6.97	0.95	0.06	8.32	0.986	13.66	0.934	0.053
$[(\text{MgO})_{62}\text{V}_0]^0$ F <sup>++</sup>	4.47	1.06	5.58	0.935	6.998	0.955	0.099	8.39	0.994	13.66	0.933	0.061

$d_{A_iA_j}$  being the distance between atoms  $A_i$  and  $A_j$ . The sphericity  $s$  is then estimated by:

$$s = 1 - \frac{\rho_{A_1A_2}}{\rho_{A'_1A'_2}}$$

where  $A_1$  and  $A_2$  are now atoms belonging to two opposite vertices, and  $A'_1$  and  $A'_2$  to two opposite face centers. The value of  $s$  increases with the sphericity of the cluster, a cubic cluster having  $s = 0$ , and a spherical one  $s = 1 - 1/\sqrt{3} = 0.42$ .

Our results are presented in Table 2. All distances are less than in the crystal, with the exception of the distance between the first two neighbours of the vacancy,  $d_{\text{Mg}_1\text{Mg}_2}$ , in five of the six vacancy clusters. The removal of electrons in a vacancy cluster leads always to an increase of the  $\text{Mg}_1\text{Mg}_2$  distance [19,21,37]. A similar result was found in  $\text{SiO}_2$  although its rather asymmetric structure: within the supercell [3] as well as within the cluster approach [25] the positive charging of an oxygen vacancy leads to a lengthening of the Si–Si bond. This effect underlines the binding part played by delocalised electrons.

For given equivalent crystal charges, small clusters are more spherical than large ones and their sphericity increases more when a neutral vacancy is created. When electrons are removed, small clusters experience an increase of their sphericity. Large clusters are composed of an inner part similar to a small cluster, embedded in an outer part. For given equivalent crystal charges, the sphericity of this inner part is less than that of the small cluster, and its variations are smaller. In the outer part, the interatomic distances remain very similar to those of the crystal (with differences less than 7%) and the sphericities less than 0.07.

These properties result from the localisation of the electronic density we shall study now.

## 5 Localisation of the electronic density

### 5.1 Mulliken charges

The DMol code provides the Mulliken charges of the atoms (*cf.* Tab. 3). Although the choice of these charges is probably not the best one<sup>1</sup>, because they can slightly underestimate the ionicities, we shall use them, and complete the information they provide by maps of the charge density and by a direct computation of the charge included in the vacancy.

#### 5.1.1 Ionicity and sphericity of the clusters

The small clusters are more ionic than the large ones. However, the valence charges (+2 for Mg and –2 for O), often assumed in MgO simulations [8,16,29,38], are never reached. In fact, in MgO clusters, the ionic charge of an atom results principally from a compromise between its coordination  $Z$  and the Madelung energy  $\varepsilon_M$  at the atom site [39]. The probability for an electron to escape an ionic site and to make covalent bounds with its neighbours is proportional to the number  $Z$  of these atoms<sup>2</sup>. So the ionic charge of an atom decreases with  $Z$ . Besides, it increases with the electrostatic energy  $\varepsilon_M$ . The most striking example of this compromise is the central oxygen atom (*cf.* Tab. 3). In both clusters its coordination is maximum ( $Z = 6$ ); however in the small cluster, the large charges of its neighbours, due to their low values of  $Z$ , give rise to a high value of  $\varepsilon_M$  at the central atomic site. In definitive,

<sup>1</sup> Hirschfeld charges and point charges available in the DMol code are not better adapted to our problem.

<sup>2</sup> The dependence of this probability with respect to the interatomic distances has been shown to be negligible in MgO clusters [39].

**Table 3.** Mulliken charges relative to some atoms of the clusters. See Figure 1 for the locations of the atoms.

		Mg <sub>1</sub>	Mg <sub>3</sub>	Mg <sub>5</sub>	Mg <sub>7</sub>	O <sub>1</sub>	O <sub>2</sub>	O <sub>4</sub>	O <sub>6</sub>	O <sub>8</sub>	O <sub>10</sub>
$[(\text{MgO})_{13}\text{Mg}]^{2+}$		1.18	1.56			-1.50	-1.34				
$[(\text{MgO})_{12}\text{Mg}_2\text{V}_0]^{2+}$	F	1.16	1.37				-1.33				
$[(\text{MgO})_{12}\text{Mg}_2\text{V}_0]^{3+}$	F <sup>+</sup>	1.17	1.53				-1.36				
$[(\text{MgO})_{12}\text{Mg}_2\text{V}_0]^{4+}$	F <sup>++</sup>	1.21	1.67				-1.39				
$[(\text{MgO})_{62}\text{O}]^{2-}$		1.10	1.02	1.22	1.30	-1.18	-1.26	-1.18	-1.17	-1.14	-1.28
$[(\text{MgO})_{62}\text{V}_0]^{2-}$	F	0.92	1.04	1.23	1.28		-1.25	-1.20	-1.17	-1.15	-1.28
$[(\text{MgO})_{62}\text{V}_0]^{1-}$	F <sup>+</sup>	1.00	1.02	1.23	1.32		-1.24	-1.21	-1.18	-1.16	-1.28
$[(\text{MgO})_{62}\text{V}_0]^0$	F <sup>++</sup>	1.07	1.02	1.23	1.34		-1.22	-1.21	-1.19	-1.17	-1.29

the determinant effect on ionicity is the coordination of the majority of atoms, or, in other words, the value  $R$  of the surface to volume ratio [9,26].

The clusters geometries are also due to this ratio  $R$ : it was already observed [9,26] that the sphericity of a MgO cluster increases with its ionicity.

### 5.1.2 Creation of the vacancy

The removal of the neutral central oxygen atom mainly affects the 8 vertices magnesium atoms in the small cluster, and its first 6 neighbours in the large one. Its negative charge is almost exactly shared between these atoms, which see their positive charge to decrease. A similar property of charge sharing was observed by Castanier and Noguera, who studied neutral surface oxygen vacancies with the help of a periodic method [40].

So, after the creation of the neutral oxygen vacancy, electrons have a tendency to run away towards the vertices atoms — which have the smallest coordination — in the small cluster whereas in the large one, they remain in the immediate vicinity of the vacancy, where they modify the charges of its first neighbours. As the charges of the other atoms remain almost unchanged in this cluster, one can foresee that charge transfers would likely be similar in a crystal.

### 5.1.3 Removal of electrons

When electrons are removed from the vacancy clusters the variations of the Mulliken charges are more important in the small cluster than in the large one. Electrons are principally taken off from the atoms which were modified by the oxygen atom removal (see last section). After the removal of two electrons, the 8 vertices atoms of the small cluster have lost more than 2 electrons, for only about 0.9 electron in the set of the first 6 neighbours of the vacancy in the large cluster. And the charge reorganisation of the large cluster remains moderate with respect to that of the small one.

So, charge localisation and transfers are very sensitive to the cluster size. In order to study them in greater details, let us introduce maps of the charge density.

## 5.2 Charge repartition and transfers

In order to visualize the reorganisation of the electronic density after the removal of one electron, the easiest method would be to calculate the difference between the electronic densities respectively associated to the cluster charges  $Q$  and  $Q + 1$ . However this method cannot be applied here, because the cluster structure varies with  $Q$ . Another method was proposed in a previous paper [26]: the charge  $Q$  of a cluster is raised to  $Q + 1$ , without modifying its geometry, and the energy minimisation is performed. The difference between the electronic densities respectively associated to  $Q$  and  $Q + 1$  provides the “vertical” changes brought by the removal of the electron, before relaxation of the cluster. The further reorganisation of the electronic density does not generally modify the Mulliken charges by more than 2%.

In Figures 3 and 4 are shown the electronic density modifications brought by the removal of one electron in a cluster equivalent to a neutral crystal. A positive density variation means a decrease of the electronic density, and a negative one an increase.

The transition  $2^+ \rightarrow 3^+$  is represented in Figure 3 in two planes of the small cluster. In the central (100) plane (Fig. 3a), the charge density variation around the oxygen atom  $\text{O}_2$  is composed of a positive inner shell surrounded by a negative one: the removal of the electron leads to the expansion of the electronic charge around  $\text{O}_2$ . Besides, a decrease of the electronic density is observed in the vacancy region, around  $\text{Mg}_1$  atoms and at the cluster periphery.

The (100) plane passing through a vertex  $\text{Mg}_3$  atom (but not exactly through  $\text{Mg}_1$  and  $\text{O}_2$ , due to the sphericity of the cluster) is represented in Figure 3b. Only the central region, around  $\text{Mg}_1$ , gains electrons; all the other atoms, ( $\text{Mg}_3$  and  $\text{O}_2$ ), as well as the periphery, lose electrons.

Removing one electron from an ionic-covalent cluster reduces the cohesion forces. In order to compensate this effect, the covalent bonds have to be increased by a transfer of a part of the localised electrons into the interatomic volume. The cluster periphery, the vacancy and the vertices atoms lose electrons. To a certain degree, the increase of the Mulliken charges of the atoms (see lines 2 to 4 of Tab. 3) indicates these variations. However, as the

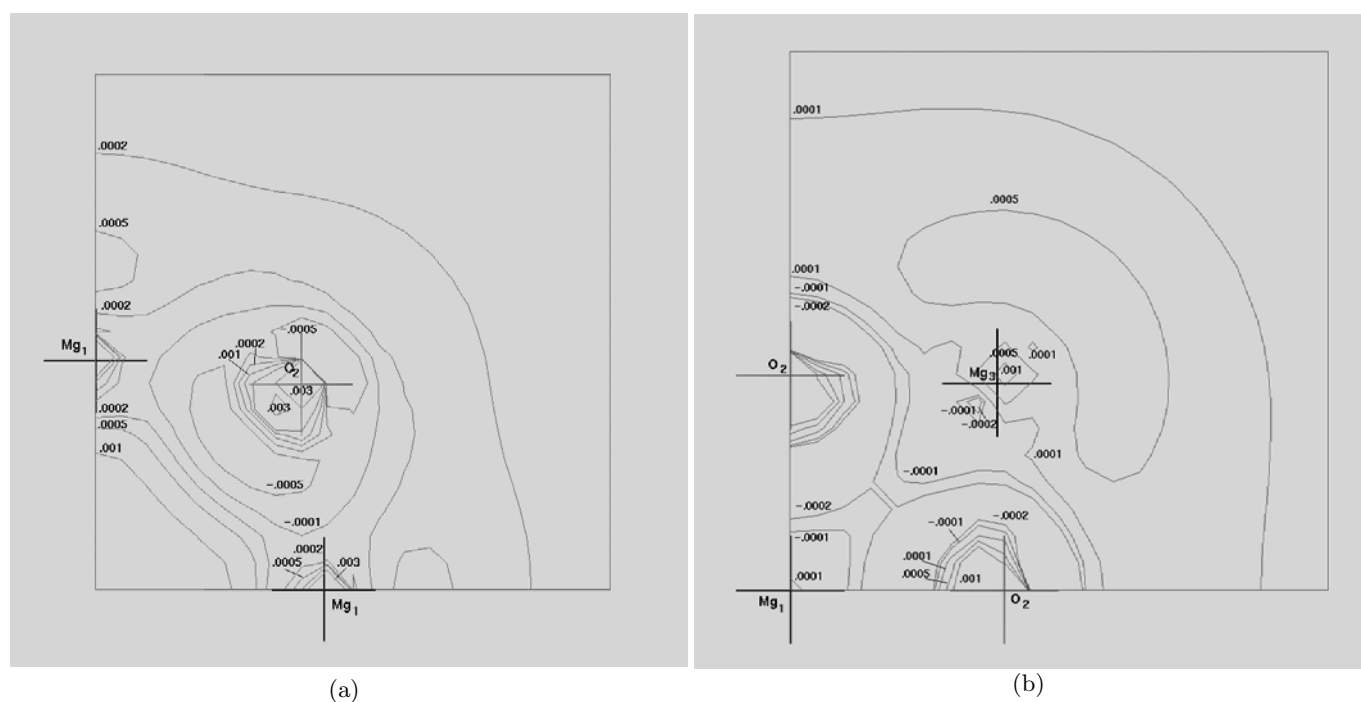


**Fig. 3.** “Vertical” variations of the electronic charge density when the charge  $Q$  of  $[(\text{MgO})_{12}\text{Mg}_2\text{V}_0]$  varies from +2 to +3 in: (a) the central (100) plane of the cluster; (b) the (100) plane passing through the vertex  $\text{Mg}_3$  atom (see Fig. 1). Only the upper right quarter of each plane is shown, the three other quarters being obtained by symmetry. The atoms are represented by crosses. When  $Q$  varies from +3 to +4, very similar variations are obtained.

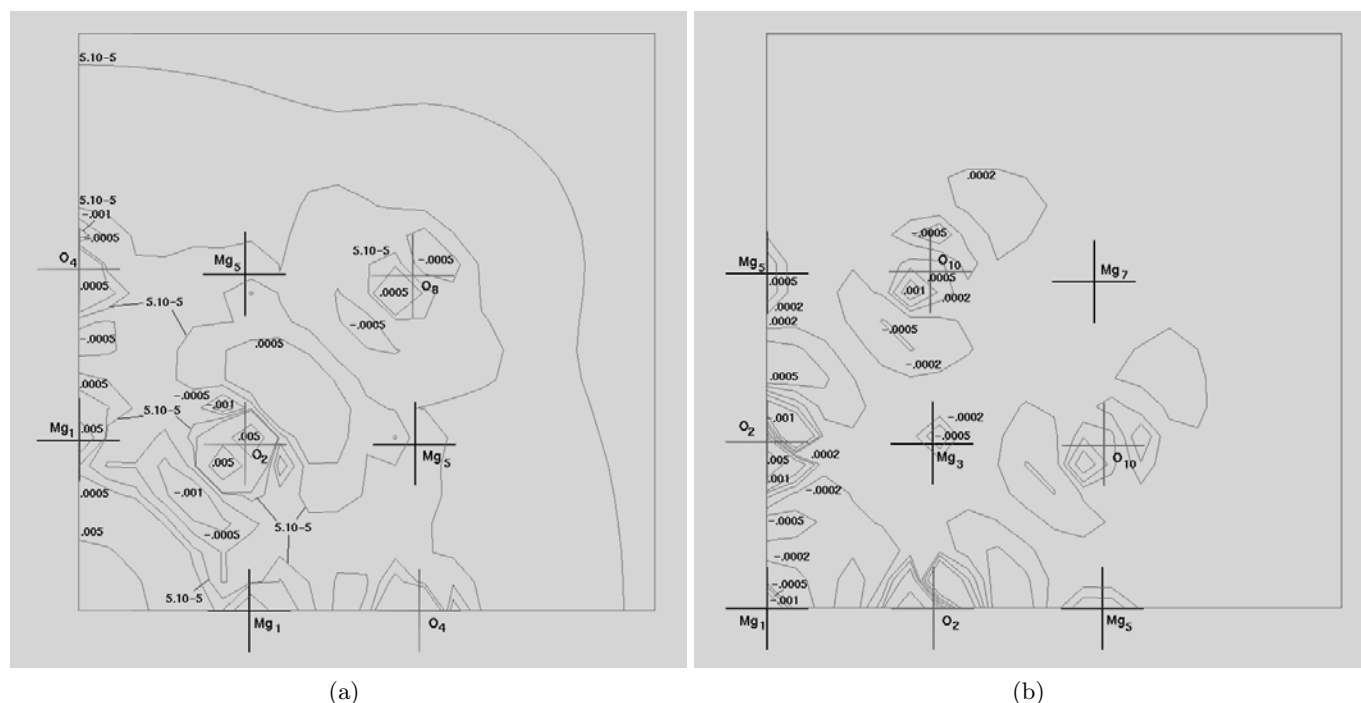


**Fig. 4.** “Vertical” variations of the electronic charge density when the charge  $Q$  of  $[(\text{MgO})_{62}\text{V}_0]$  varies from -2 to -1 in (a) the central (100) plane of the cluster, (b) the (100) plane passing through a  $\text{Mg}_3$  atom (see Fig. 1). Only the upper right quarter of each plane is shown, the three other quarters being obtained by symmetry. The atoms are represented by crosses. When  $Q$  varies from -1 to 0, very similar variations are obtained.

Mulliken charges take into account localised as well as delocalised electrons, their values do not exactly follow the ionicity changes.

The central (100) plane and the (100) plane passing through a  $\text{Mg}_3$  atom in the large cluster are represented in Figure 4, for a transition  $2^- \rightarrow 1^-$  (equivalent to the previous transition  $2^+ \rightarrow 3^+$ ). At the periphery of the cluster and in the vicinity of  $\text{Mg}_1$  belonging to this plane, the decrease of the charge density is very small (about  $5 \times 10^{-5} e/\text{cm}^3$ ) and does not appear in the figures. The vacancy, the oxygen atoms and some magnesium atoms see their electronic density to decrease. The remaining electrons have to strengthen the cluster cohesion by occupying the interatomic space. Figure 4b shows a large domain comprised between  $\text{Mg}_3$  (central in the figure) and  $\text{Mg}_1$  which receives an important electron amount.

Along the  $\langle 110 \rangle$  axis passing through the vacancy (*cf.* Fig. 4a), the electronic density increases between the vacancy and  $\text{O}_2$ , and decreases between  $\text{O}_2$  and  $\text{O}_8$ . This asymmetrical variation is probably due to a charge transfer between the vacancy and  $\text{O}_2$  and it must give rise to an important change of the induced dipole moment on the atom  $\text{O}_2$ . This polarisation effect, which was not observed in the small cluster, would likely occur around a positively charged vacancy in a crystal.

When a second electron is removed, the same tendencies are observed.

### 5.3 Charge localised in the vacancy

The problem of the charge localised in the vacancy is delicate, due to the anisotropy of the electronic charge (see Figs. 3 and 4 for instance). What volume has to be assigned to the vacancy [8, 21, 23, 41]? The simplest idea is to assimilate the vacancy to a sphere which radius  $r_v$  can be estimated from the distance  $d_{\text{Mg}_1\text{Mg}_2}$  and from the ionic radius of magnesium  $r_i^{\text{Mg}}$ , by:

$$d_{\text{Mg}_1\text{Mg}_2} = 2r_i^{\text{Mg}} + 2r_v. \quad (1)$$

The ionic charge of magnesium atoms being nearer from +1 than from +2 (*cf.* Tab. 3), the value  $r_i^{\text{Mg}} = 0.82 \text{ \AA}$  associated to  $\text{Mg}^+$  [42] can be chosen. As  $d_{\text{Mg}_1\text{Mg}_2}$  is a function of the total charge  $Q$ , the vacancy size depends on  $Q$ . In Table 4 are given the values of  $r_v$  (*cf.* Eq. (1) and Tab. 2) and the charges  $Q_v$  included in the spheres of radius  $r_v$ . The consequence of the removal of one electron is to increase  $r_v$  by about 3% in the small cluster, 6% in the large one.

The values of  $Q_v$  are very sensitive to the values of  $r_v$ . The last column of Table 4 gives the charges  $Q'_v$  which would have been found if the radius of the vacancy was kept fixed. In  $[(\text{MgO})_{62}\text{V}_0]^0$ , if the radius  $r_v = 1.25 \text{ \AA}$  was chosen, the difference would reach more than 40%! In fact, if the charge density was homogeneous, an increase  $\delta r_v$  of  $r_v$  would lead to an increase  $\delta Q_v$  of  $Q_v$  such as  $\delta Q_v/Q = 3\delta r_v/r_v$ . Here  $\delta r_v/r_v \sim 0.13$ , so one would obtain  $\delta r_v/r_v \sim 0.39$ . Therefore, a radius varying with  $Q$  has to be considered.

**Table 4.** Radius  $r_v$  of the vacancy, charge  $Q_v$  included in a sphere of radius  $r_v$  centered on the vacancy, charge  $Q'_v$  included in a sphere of radius  $1.40 \text{ \AA}$  in the small cluster, and of radius  $1.25 \text{ \AA}$  in the big one. The electron charge  $e$  is the unit used for  $Q_v$  and  $Q'_v$ .

		$r_v \text{ \AA}$	$Q_v$	$Q'_v$
$[(\text{MgO})_{12}\text{Mg}_2\text{V}_0]^{2+}$	F	1.40	0.89	
$[(\text{MgO})_{12}\text{Mg}_2\text{V}_0]^{3+}$	$\text{F}^+$	1.44	0.80	0.71
$[(\text{MgO})_{12}\text{Mg}_2\text{V}_0]^{4+}$	$\text{F}^{++}$	1.49	0.73	0.54
$[(\text{MgO})_{62}\text{V}_0]^{2-}$	F	1.25	1.09	
$[(\text{MgO})_{62}\text{V}_0]^{1-}$	$\text{F}^+$	1.325	0.91	0.75
$[(\text{MgO})_{62}\text{V}_0]^0$	$\text{F}^{++}$	1.415	0.64	0.35

In the clusters equivalent to the neutral vacancy crystal (F-center), at most only about one electron is located in the vacancy, the other one is anisotropically spread in the rest of the cluster. In the small cluster, more ionic than the large one,  $Q_v$  is less and its variations with  $Q$  less rapid because electrons are more localised in the vicinity of atoms, and have a less tendency to extend towards the vacancy. When two electrons are removed ( $\text{F}^{++}$ ), the vacancy still contains about two thirds of electron in both clusters.

These results are very different from the classical representation of the F,  $\text{F}^+$  and  $\text{F}^{++}$  centers where the vacancy respectively contains 2, 1 and 0 electrons. Computations made by Michèle Gupta [43] with the help of a APW method lead to a conclusion similar to ours: assigning a radius  $1.25 \text{ \AA}$  to the neutral vacancy, she obtained 0.94 electrons in the volume so defined.

Similarly to the charge of an atom in a solid for which many definitions were given (*e.g.* Mulliken, Hirschfeld...), the volume of the vacancy can be defined in many ways. For instance, the vacancy can be considered as a non nuclear attractor, which gives rise to a local basin of attraction [44, 45]. Starting from the cube center, the minima of the lines of steepest descent of the electronic density define the boundaries of the vacancy. This method provides values of  $Q_v$  larger than ours. The computations of Paula Mori-Sánchez *et al.* [46] for F and  $\text{F}^+$  centers show that the difference results principally from the interatomic volumes, which are considered as belonging either to the vacancy, or to its neighbouring atoms.

Another point of view is to use non local methods [47] in order to obtain the amount of delocalisation of the electron. In the next section we shall qualitatively associate this quantity to the location of the vacancy levels in the bandgap.

## 6 Energetics

### 6.1 Energies relative to cohesion and to vacancy formation

Amongst the quantities which have been experimentally measured, the cohesive energy per molecule  $E_c$  and the

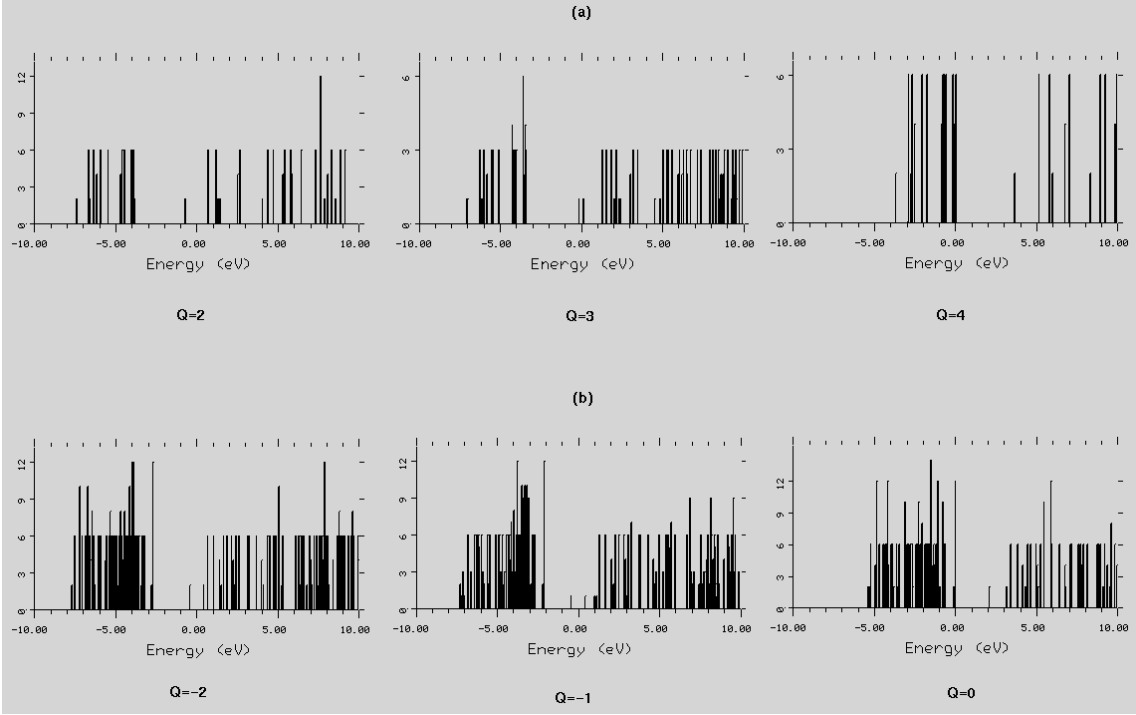


**Fig. 5.** Density of states of (a)  $[(\text{MgO})_{12}\text{Mg}_2\text{V}_0]^Q$  and (b)  $[(\text{MgO})_{62}\text{V}_0]^Q$ . The origin of energies is taken at the Fermi level. The height of the levels is proportional to their degeneracy, with a resolution of 0.01 eV.

**Table 5.** Gap  $\Delta$ , total energy  $E_{\text{tot}}$ , binding energy  $E_b$  and ionisation potential IP of each cluster.

		$\Delta(\text{eV})$	$E_{\text{tot}}$ (a.u.)	$E_b(\text{eV})$	IP (eV)
$[(\text{MgO})_{13}\text{Mg}]^{2+}$		3.66	-3761.056	113.66	13.55
$[(\text{MgO})_{12}\text{Mg}_2\text{V}_0]^{2+}$	F	4.51	-3686.148	103.51	10.61
$[(\text{MgO})_{12}\text{Mg}_2\text{V}_0]^{3+}$	F <sup>+</sup>	4.73	-3685.758	92.90	13.66
$[(\text{MgO})_{12}\text{Mg}_2\text{V}_0]^{4+}$	F <sup>++</sup>	5.15	-3685.256	79.24	21.36
$[(\text{MgO})_{62}\text{O}]^{2-}$		2.99	-17066.3454	656.201	2.40
$[(\text{MgO})_{62}\text{V}_0]^{2-}$	F	3.11	-16991.3905	644.788	0.02
$[(\text{MgO})_{62}\text{V}_0]^{1-}$	F <sup>+</sup>	3.08	-16991.3897	644.767	2.63
$[(\text{MgO})_{62}\text{V}_0]^0$	F <sup>++</sup>	3.15	-16991.2931	642.139	6.41

vacancy formation energy  $E_f$  have been particularly studied [19,21,24,29,40,41]. For the small cluster these energies were computed in reference [26]:  $E_c = 8.84$  eV and  $E_f = 10.16$  eV.

For the large cluster, our computation provides:  $E_f = 11.42$  eV (energy of  $[(\text{MgO})_{62}\text{O}]^{2-}$  minus the sum of the energies of the neutral oxygen atom and of  $[(\text{MgO})_{62}\text{V}_0]^{2-}$ ) and  $E_c = 10.40$  eV (binding energy of  $[(\text{MgO})_{62}\text{V}_0]^{2-}$  divided by the number of molecules).

In MgO crystals, the experimental values of  $E_f$  and  $E_c$  have been found to be 11.875 and 10.345 eV respectively [48,49]. The results we obtained in the small cluster are both too low; in the large one, they only differ from the experimental values by less than 4% for  $E_f$  and 6% for  $E_c$ . These results illustrate the influence of the cluster size, or, more precisely, of its surface to volume ratio  $R$  (see similar results in Refs. [50,51] for small NaCl and LiH clusters for instance).

## 6.2 Density of states and gaps

The values  $\Delta$  of the gaps, given in Table 5, are higher in the small cluster than in the large ones. The oxygen atom removal always produces an increase of  $\Delta$ , which attains 25% in the small cluster against only about 4% in the large one. These properties are due to the more important increase of  $R$  (*cf.* Sect. 5.1.1) in the small cluster than in the large one [41,52].

When electrons are removed, the value of  $R$  is constant. However the variations of  $\Delta$  attain 25% in the small cluster, whereas they remain less than 3% in the other one. Now, these variations are likely due to the ionicity variations: the ionic charges increase for all atoms in the small cluster, whereas in the large one, they increase, decrease or remain constant according to the atoms localisations (*cf.* Tab. 3 and Sect. 5.1.1). If the real gap of the large cluster was very near that of a crystal, that is about

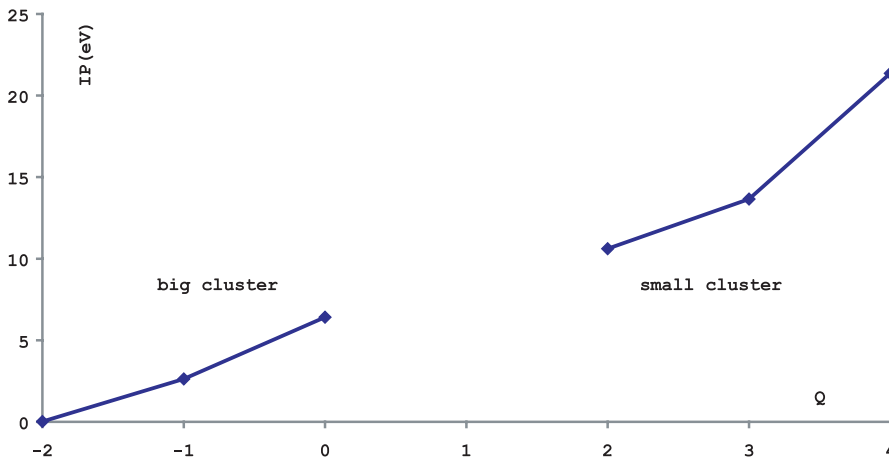


**Fig. 6.** Adiabatic ionisation potentials IP as a function of the total cluster charge  $Q$ . The lines are only intended as a guide.

8 eV [53], the LDA method would only provide about 40% of this value. Then if the underestimation was the same in all clusters, the real gap in small clusters would be of the order of 11 to 12 eV, which is a plausible estimate due to their larger ionicity.

Figures 5a and 5b show the densities of states of the vacancy clusters, the origin of the energies being the Fermi level. The removal of an electron always leads to a modification of all levels.

Let us consider the vacancy levels included in the gaps. When two electrons are present (neutral state), the level is unique but doubly degenerated: the two spin states are filled. This level is below the Fermi level, nearer from the conduction than from the valence band: its distance to the “conduction band”, 1.39 and 0.85 eV in small and large cluster respectively, represents 30.7% and 27.4% of the bandgap (see Tab. 5): this results from the delocalisation of the vacancy electrons previously pointed out. The fact that the level is proportionally nearer from the conduction band in the small cluster than in the large one is probably non significant, due to the spreading of levels in the small cluster (see Fig. 5a).

When one electron is removed, the degeneracy is split. The Fermi level is between the two vacancy levels. The energy of the second electron is lowered: its distance to the bottom of the conduction band is now 1.46 eV in the small cluster, and 1.45 eV in the large one, *i.e.* respectively 30.9% and 46.9% of the bandgap (see Tab. 5). This shows that the influence of the removal of the first electron on the second one is less in the small cluster than in the large one. The reason is probably a larger delocalisation of these electrons in the small cluster, leading to a less repulsion between them. Now, the unoccupied level plays the part of an excited state, at 0.27 eV above the ground state in the small cluster, at 0.88 eV in the large one.

If the second electron is removed, the level is doubly degenerate and empty. It is now located above the Fermi level at 1.50 eV from the bottom of the conduction band in the small cluster, and at 1.06 eV in the large one (29.2% and 33.7% of the gap). This level can be considered as a virtual excited level, occupied only transitorily in processes for which the characteristic transition time would be

less than the relaxation time of the system (for instance in a multiphoton transition). A transition towards this level would provide a very diffuse line, to the contrary of the narrow lines which would be observed in the transitions occurring when only one electron has been removed.

Although our method can provide only qualitative estimates concerning these levels, our results are relatively similar to those of Klein *et al.* [28] obtained by band structure calculations. The results relative to embedded clusters are very sensitive to the computational method: Gibson *et al.* [18] situate the F-center level at a distance from the conduction band representing 18.85% of the gap, when Ferrari and Pacchioni [19] find the same level approximately in the middle of the bandgap. A recent experimental paper [54] leads to the conclusion that  $F^+$  centers are very stable in  $Al_2O_3$ . Is it the same in  $MgO$ ?

### 6.3 Ionisation potentials

In Table 5 are indicated some clusters energies. According to the cluster sizes, the ionisation potentials IP are very different. Typically 10 to 20 eV in the small clusters against 2.5 to 5 eV in the large ones. The creation of a vacancy leads to a decrease of IP: as the attractive central potential is suppressed, all states see their energies to increase, and the removal of an electron is more easy.

In vacancy clusters, the variations of IP with respect to the total cluster charge  $Q$  are illustrated in Figure 6. As in other computations [19, 21], a general increase of IP with  $Q$  appears, giving rise to larger values in the small than in the large cluster; besides, the slope of the curve increases more rapidly in the small cluster than in the large one. These trends cannot result from differences in the Madelung energy due to the vacancy charge, because in the small cluster, the vacancy charge is always less than in the large cluster and experiences smaller variations (*cf.* Tab. 4). They are due to the increase of Coulomb interactions: for increasing values of  $Q$ , the electronic repulsion decreases and the ionisation energy increases. This effect is similar to that described by the Hubbard energy in atoms.



This increase of IP with  $Q$  is quite linear when the cluster loses one and two electrons. Then an increase of the slope appears when the vacancy is empty, or almost empty (see Tab. 4). The states in the bandgap being empty too, the escaping electron has to jump the totality of the bandgap. As the bandgap is larger in the small cluster than in the large one, the increase of IP is more important. The variations of IP can be related to the fact that the departing electron is more localised in the valence band than in the vacancy level, and in the small cluster than in the large one [55,56].

These results can be compared to those of Ferrarri and Pacchioni [19] concerning two embedded clusters of different sizes with a surface vacancy:  $[(\text{MgO})_{12}\text{MgV}_0]^Q$  and  $[(\text{MgO})_{20}\text{MgV}_0]^Q$ . The values of IP respectively associated to F and  $\text{F}^+$  centers are: 5.39 and 11.17 eV for the small cluster ( $Q = 0$  and  $Q = 1$ ) and 4.71 and 9.69 eV for the large one ( $Q = 0$  and  $Q = 1$ ). They increase with  $Q$  and decrease with the cluster size as in our computation. The decrease of IP with the size of the cluster is probably due to a decrease of its ionicity. However, for a precise comparison with our clusters, the influence of the surrounding point charges would have to be taken into account.

## 7 Conclusion

Two sizes of charged MgO clusters have been simulated in this paper. Similarities between the two sizes have been pointed out, the main similarity being that a neutral oxygen vacancy does not accept more than about one electron and, that after the removal of two electrons, it is not completely empty, but still contains about two thirds of electron. On the other hand, very important electronic properties have been found to be size dependent. For instance, the ionicity which seems to be strongly related to the surface to volume ratio or the charges transfers occurring in vacancy clusters when electrons are removed.

These properties show that, in order to study a vacancy in a crystal, the small cluster cannot be used, but that the inner part of the large cluster seems to be a good candidate. Let us recall, for instance, that, in the non-vacancy cluster, the Mulliken charges of this inner part do not differ by more than 13% from their values in the crystal ( $\pm 1.12$ ) [39], and that the outer part is not very far from a crystalline cube (see Sect. 4).

So if the assumption is done that the inner part of the large cluster is very similar to the immediate vicinity of a vacancy in a crystal, some properties can be proposed for a crystal possessing oxygen vacancies, in any case a deformation of the crystal around each vacancy, and, when the crystal is positively charged,

- an increase of this deformation,
- a reorganisation of the electronic density leading to a slight decrease of the electronic charge of the magnesium atoms first neighbours of the vacancy,
- polarisation effects in the immediate vicinity of vacancies, principally along the  $\langle 110 \rangle$  directions,
- a narrow excited state associated to the vacancies,

- a greater conductivity due to the presence of the vacancy levels: according to its initial level, an electron has to gain 0.85, 1.445 or 3.15 eV to reach the conduction band (see Sect. 6.2). Although these values, obtained by a DFT-LDA method, are probably underestimated by more than 50%, they allow to understand that a crystal containing vacancies and subjected to progressive positive charging will give rise successively (and simultaneously) to the three types of processes. This situation can be compared to that of a semi-conductor, vacancies playing the part of defects.

## References

1. For instance see P. Joyes, *Monographie de Physique: Les Agrégats Inorganiques Élémentaires* (Éditions de Physique, Paris, 1990)
2. M.R. Hayns, L. Dissado, *Theoret. Chim. Acta* **37**, 147 (1975)
3. J.K. Rudra, W. Beall Fowler, *Phys. Rev. B* **35**, 8223 (1987)
4. W.A. Saunders, *Phys. Rev. B* **37**, 6583 (1988)
5. W.A. Saunders, *Z. Phys. D* **12**, 601 (1989)
6. A. Pandey, J.M. Vail, *J. Phys. Cond. Matt.* **1**, 2801 (1989)
7. R.W. Grimes, R.A. Catlow, A. Marshall Stoneham, *J. Chem. Soc. Faraday Transl. 2* **85**, 485 (1989)
8. J.M. Vail, *J. Phys. Chem. Sol.* **51**, 589 (1990)
9. P.J. Ziemann, A.W. Castleman Jr, *J. Chem. Phys.* **94**, 718 (1991)
10. P.J. Ziemann, A.W. Castleman Jr, *Phys. Rev. B* **44**, 6488 (1991)
11. P.J. Ziemann, A.W. Castleman Jr, *Z. Phys. D* **20**, 97 (1991)
12. A.V. Bezel', V.A. Lobach, *Sov. Phys. Sol. State* **33**, 744 (1991)
13. C. Bréchnignac, Ph. Cahuzac, F. Carlier, M. de Frutos, J. Leygnier, *J. Ph. Roux, J. Chem. Phys.* **99**, 6848 (1993)
14. J.M. Recio, R. Pandey, A. Ayuela, A.B. Kunz, *J. Chem. Phys.* **98**, 4783 (1993)
15. J.M. Recio, R. Pandey, *Phys. Rev. A* **47**, 2075 (1993)
16. G. Pacchioni, C. Sousa, F. Illas, F. Parmigiani, P.S. Bagus, *Phys. Rev. B* **48**, 11573 (1993)
17. S. Veliah, R. Pandey, Y.S. Li, J.M. Newsam, B. Vessal, *Chem. Phys. Lett.* **235**, 53 (1995)
18. A. Gibson, R. Haydock, J.P. LaFemina, *Phys. Rev. B* **50**, 2582 (1994)
19. A.-M. Ferrari, G. Pacchioni, *J. Phys. Chem.* **99**, 17010 (1995)
20. W.C. Mackrodt, R.F. Stewart, *J. Phys. C* **10**, 1431 (1977)
21. E. Scorza, U. Birkenheuer, C. Pisani, *J. Chem. Phys.* **107**, 9645 (1997)
22. F. Illas, G. Pacchioni, *J. Chem. Phys.* **108**, 7835 (1998)
23. S. Veliah, Kai-hua Xiang, R. Pandey, J.M. Recio, J.M. Newsam, *J. Phys. Chem. B* **102**, 1126 (1998)
24. P.V. Sushko, A.L. Shluger, C. Pichard, A. Catlow, *Surf. Sci.* **450**, 153 (2000)
25. A.C. Pineda, S.P. Karna, *J. Phys. Chem. A* **104**, 4699 (2000)
26. C. Coudray, G. Blaise, M.J. Malliavin, *Eur. Phys. J. D* **11**, 127 (2000)
27. M.J. Malliavin, C. Coudray, *J. Chem. Phys.* **106**, 2323 (1997)

28. B.M. Klein, W.E. Pickett, L.L. Boyer, R. Zeller, *Phys. Rev. B* **35**, 5802 (1987)
29. Q.S. Wang, N.A.W. Holzwarth, *Phys. Rev. B* **41**, 3211 (1990)
30. A. De Vita, M.J. Gillan, J.S. Lin, M.C. Payne, I. Štich, L.J. Clarke, *Phys. Rev. B* **46**, 12964 (1992)
31. M. Boero, A. Pasquarello, J. Sarnthein, R. Car, *Phys. Rev. Lett.* **78**, 887 (1997)
32. P. Hohenberg, W. Kohn, *Phys. Rev. B* **136**, 864 (1964)
33. W. Kohn, L.J. Sham, *Phys. Rev. A* **140**, 1133 (1965)
34. B. Delley, *J. Chem. Phys.* **92**, 508 (1990)
35. B. Delley, *J. Chem. Phys.* **94**, 7245 (1991)
36. L. Hedin, B.I. Lundqvist, *J. Phys. C* **4**, 2064 (1971)
37. In crystalline MgO a similar result was obtained as soon as 1967 by W.P. Unruh, J.W. Culvahouse, *Phys. Rev.* **154**, 861 (1967)
38. R.W. Grimes, C.R.A. Catlow, A.M. Stoneham, *J. Phys. Cond. Matt.* **1**, 7367 (1989)
39. S. Moukouri, thesis, Orsay, 1993
40. E. Castanier, C. Noguera, *Surf. Sci.* **364**, 1 (1996)
41. L.N. Kantorovich, J.M. Holender, M.J. Gillan, *Surf. Sci.* **343**, 221 (1995)
42. *CRC Handbook of Chemistry and Physics*, 72nd edn. (CRC Press, Boca Raton, 1992), pp. 12-8
43. M. Gupta, private communication
44. R.F.W. Bader, *J. Chem. Phys.* **73**, 2871 (1980)
45. B. Silvi, A. Savin, *Nature* **371**, 683 (1994)
46. P. Mori-Sánchez, J.M. Recio, B. Silvi, C. Sousa, A. Martin Pendas, V. Luaña, F. Illas, *Phys. Rev. B* **66**, 075103 (2002)
47. A.D. Becke, K.E. Edgecombe, *J. Chem. Phys.* **92**, 5397 (1990)
48. *CRC Handbook of Chemistry and Physics*, 60th edn. (CRC Press, Boca Raton, 1980), p. D-72
49. L. Kappers, R. Kroes, E. Hensley, *Phys. Rev. B* **1**, 4150 (1970)
50. A. Ayuela, J.M. López, J.A. Alonso, V. Luaña, *Physica B* **212**, 329 (1995)
51. M. Bertolus, V. Brenner, P. Millié, *J. Chem. Phys.* **115**, 4070 (2001)
52. U. Schönberger, F. Aryasetiawan, *Phys. Rev. B* **52**, 8788 (1995)
53. D.M. Roessler, W.C. Walker, *Phys. Rev.* **159**, 733 (1967)
54. P. Jonnard, C. Bonnelle, G. Blaise, G. Remond, C. Roques-Carnes, *J. Appl. Phys.* **88**, 6413 (2000)
55. P. Labastie, J.M. L'Hermite, Ph. Poncharal, M. Sence, *J. Chem. Phys.* **103**, 6362 (1995)
56. Ph. Poncharal, J.M. L'Hermite, P. Labastie, *Chem. Phys. Lett.* **253**, 463 (1996)